Erratum

Strategies of actin reorganisation in plant cells

Andrei P. Smertenko, Michael J. Deeks and Patrick J. Hussey

Journal of Cell Science 123, 3029

doi:10.1242/jcs.079749

There were errors published in the e-press version of *J. Cell Sci*. **123**, 3019-3028.

In the Introduction, on page 3019, the second last sentence is incorrect.
The correct sentence should read:
New filaments can be assembled from shorter free cytoplasmic filaments, from the products of F-actin severing and by polymerisation from the ends of extant filaments.

On page 3027, left column, second paragraph, the third sentence incorrectly contains the word ‘after’ immediately before the word ‘separation’.
The correct sentence should read:
For example, the frequency of rings or acquosomes decreases in an aging tobacco BY-2 cell culture (Hasezawa et al., 1988), increases during heat-stress (Chaidee at al., 2008) and following mechanical separation of Zinnia mesophyll cells (Frost and Roberts, 1996).

On page 3027, left column, second paragraph, ninth line from bottom.
The number of acquosomes is reduced by 98.9%, and not, as incorrectly stated, by 98%.
We apologise for these mistakes.

Strategies of actin reorganisation in plant cells

Andrei P. Smertenko, Michael J. Deeks and Patrick J. Hussey*

School of Biological and Biomedical Sciences, University of Durham, South Road, Durham DH1 3LE, UK

*Author for correspondence (p.j.hussey@durham.ac.uk)

Accepted 24 May 2010
Journal of Cell Science 123, 3019-3028

doi:10.1242/jcs.071126

Summary

Spatial-temporal flexibility of the actin filament network (F-actin) is essential for all basic cellular functions and is governed by a stochastic dynamic model. In this model, actin filaments that randomly polymerise from a pool of free actin are bundled with other filaments and severed by ADF/cofilin. The fate of the severed fragments is not known. It has been proposed that the fragments are disassembled and the monomeric actin recycled for the polymerisation of new filaments. Here, we have generated tobacco cell lines and *Arabidopsis* plants expressing the actin marker Lifeact to address the mechanisms of F-actin reorganisation in vivo. We found that F-actin is more dynamic in isotropically expanding cells and that the density of the network changes with a periodicity of 70 seconds. The depolymerisation rate, but not the polymerisation rate, of F-actin increases when microtubules are destabilised. New filaments can be assembled from shorter free cytoplasmic fragments, from the products of F-actin severing and by polymerisation from the ends of extant filaments. Thus, remodelling of F-actin might not require bulk depolymerisation of the entire network, but could occur via severing and end-joining of existing polymers.

Key words: Actin, Lifeact, Actin dynamics, Acquosome

Introduction

Microfilaments and microtubules are essential for a variety of cellular processes, including cell division, intracellular transport, maintaining cell architecture, isotropic and anisotropic cell expansion, response to environmental stimuli and pathogen attack. Microfilaments are formed by a globular monomeric protein actin, which exists in unpolymerised (G-actin) and polymerised (F-actin) forms. The F-actin networks within plant cells characterise the different modes of cell expansion. During anisotropic expansion of plant cells (e.g. root and hypocotyls), the majority of actin filaments are aligned parallel to the direction of expansion, and the microtubules in the cortical region of these cells are transverse. Mutations in the actin-nucleating proteins of the Arp2/3 complex and its activator SCAR/WAVE cause a reduction in cell elongation (Qian et al., 2009). In the tip-growing root hairs and pollen tubes, prominent actin fibres extend almost to the growing tip and terminate about 5 μm behind it. The apical region is occupied by vesicles delivering material that is required for cell elongation, and a network of fine filaments directs vesicle movement (Lancelle and Hepler, 1992; Hepler et al., 2001; Miller et al., 1999; Zhang et al., 2010). Destabilisation of F-actin induced by low concentration of drugs does not affect vesicle transport, but inhibits their delivery to the growing tip, causing loss of the original growth direction (Ketelaar et al., 2003). Isotropic expansion has been studied extensively in leaf pavement cells. These cells expand diffusely at first and then form protrusions that interdigitate in a jigsaw-like pattern. Here, actin filaments are randomly orientated with a concentration at the tip of expanding lobes. Mutations in proteins of the Arp2/3 complex and its activator SCAR/WAVE cause loss of interdigitation (for a review, see Qian et al., 2009); however, cell size is not significantly affected. From these data, it is reasonable to suggest that the events leading to a particular expansion mode control the dynamic parameters of F-actin organisation.

Analysis of actin organisation in cells is dependent on the development of efficient probes. Several probes have been used to date. The actin-binding domain of mouse talin (Tn) (Kost et al., 1998) allowed the observation of fine actin organisation in all plant tissues and led to a better understanding of F-actin organisation during plant development and morphogenesis (Mathur et al., 1999; Fu et al., 2001; Ilgenfritz et al., 2003; Ketelaar et al., 2004; Weerasinghe et al., 2005). This probe, however, exhibited a number of side effects (Ketelaar et al., 2004; Holweg, 2007; Wilsen et al., 2006). Another probe, the second actin-binding domain of *Arabidopsis* fimbrin 1 (fABD2) (Ketelaar et al., 2004; Sheahan et al., 2004; Voigt et al., 2005), possessed no obvious toxicity to plants and was used to measure dynamic behaviour of actin filaments in vivo (Staiger et al., 2009). Recently, a new probe called Lifeact has been generated and this is derived from the *Saccharomyces cerevisiae* actin-binding protein Abp140 (Riedl et al., 2008). Lifeact comprises the first 17 N-terminal amino acids of Abp140 and has a higher affinity for G-actin compared with F-actin. An extensive array of experiments have demonstrated that Lifeact has no apparent effect on actin dynamics in vitro, nor on the binding of several actin-associated proteins and does not appear to affect normal cell function. Lifeact has been used to visualise F-actin in budding yeast, in different mammalian cells (Riedl et al., 2008) and plant species (Era et al., 2009; Vidali et al., 2009).

Microfilaments and microtubules can coincide spatially and they have complementary roles in many cellular events (reviewed in Collings, 2008). For example, microtubules generate the architectural identity of the cytoskeletal arrays that appear in the successive stages of M-phase and these are functionally supported by microfilaments (Claydon and Lloyd, 1985; Schmit and Lambert, 1987; Traas et al., 1987; Sano et al., 2005; Higaki et al., 2008), whereas in the tip-growing root hairs and pollen tubes, the microfilament array is essential and microtubules perform a supporting role (Ketelaar et al., 2003). Several proteins can potentially crosslink microfilaments and microtubules (for a review, see Petrasek and Schwarzerova, 2009; Deeks et al., 2010), facilitating their structural and functional cooperation.

Journal of Cell Science

The dynamic behaviour of microtubules and F-actin is controlled by different mechanisms. Microtubules undergo dynamic instability, a process in which individual microtubules consecutively switch between growth, shrinking and pausing phases (reviewed in Desai and Mitchison, 1997). The switch between phases usually occurs at the dynamic plus-end of microtubules depending on the nucleotide bound to the tubulin dimer and the activity of microtubule-binding proteins. The fundamental behaviour of microtubules in vivo can be reconstituted in vitro using purified tubulin, although with different kinetic parameters, indicating that dynamic instability is an intrinsic property of microtubules that is fine-tuned by regulating proteins in vivo. Much less is known about the dynamics of F-actin in vivo. Recent observations have suggested a stochastic dynamic model, in which randomly formed actin filaments are strengthened by the spontaneous side-association of other filaments to form thicker cables, which can then elongate and get severed randomly (Michelot et al., 2007). The severed products diffuse rapidly in the cytoplasm (Staiger et al., 2009), but their fate remains unknown. The extent to which the dynamic instability of microtubules affects the stochastic dynamics of F-actin in vivo and vice versa remains unclear.

In this paper, we have generated stable lines of *Arabidopsis* plants and tobacco BY-2 tissue culture cells expressing Lifeact fused to GFP. Expression of the GFP-Lifeact construct has no discernible effect on growth and reproduction and has allowed the visualisation of actin filaments at all stages of the cell cycle and in all plant tissues examined. Using confocal laser-scanning microscopy (CLSM) and total internal reflection fluorescence microscopy (TIRF) we have addressed the fate of actin fragments after severing, the relationship between microtubule and actin dynamics and the dynamics of actin filaments in cells undergoing different modes of expansion. Our data demonstrate a new mechanism of actin network remodelling that occurs via the recycling of fragments produced as a result of severing events. This mechanism requires no bulk disassembly of filaments.

Results

Lifeact is a versatile marker of F-actin in plants

The Lifeact sequence has been linked to the 3′-end of the GFP coding sequence in the pMDC43 vector and the resulting construct transformed into *A. thaliana* plants. Thirteen individual T0 lines were isolated: in nine lines, F-actin was stained in all cells examined, in three lines, only individual cells or groups of cells were stained, and in the remaining line only cytoplasmic fluorescence and no F-actin decoration was observed. None of the lines exhibited a discernible mutant phenotype in terms of their growth and morphology compared with the wild type and plants transformed with vector only. A typical localisation of the GFP-Lifeact probe in different cell types of *A. thaliana* is shown in supplementary material Fig. S1A-D. In the tip of growing root hairs, only actin patches, short rods and cytoplasmic staining were observed, whereas in non-growing root hairs, long filaments extended to the very tip (supplementary material Fig. S1C insets).

The binding dynamic of GFP-Lifeact on F-actin was measured by fluorescence recovery after photobleaching (FRAP) in pavement leaf cells of 6-week-old seedlings. The turnover time ($t_{1/2}$) was found to be 2.56±0.70 seconds (n=10) with individual values ranging from 1.43 to 3.72 seconds. The relatively high standard deviation presumably reflects the different degrees of bundling in the actin filaments: whereby the thicker bundles will be expected to exchange GFP-Lifeact at a slower rate compared with thinner bundles as a result of steric constraints. Transient transfection of *Nicotiana benthamiana* leaves by infiltration with Agrobacterium harbouring the GFP-Lifeact construct resulted in groups of cells where the actin network was decorated similarly to stably transformed *Arabidopsis* (supplementary material Fig. S1E).

The localisation of GFP-Lifeact through the cell cycle was analysed in stably transformed *Nicotiana tabacum* BY-2 cell lines. The interphase F-actin array is an irregular dense meshwork of filaments (supplementary material Fig. S2A) organised in three interconnected domains: cortical filaments, cytoplasmic strands and a perinuclear basket (supplementary material Fig. S2B and inset). The optical (Z) sections of cells in Fig. 2A,B are shown in supplementary material Movie 1. In prometaphase, actin formed a ring of parallel filaments in the cortical layer of cytoplasm spanning around the nucleus that was similar to the pre-prophase band of microtubules (supplementary material Fig. S2C). During M-phase, the cortical F-actin formed a ‘twin-peak’ structure (Sano et al., 2005), with a clear zone in the plane of future cell division and a diffuse signal in the mitotic spindle (supplementary material Fig. S2D). We measured the fluorescence signal in the region corresponding to the centre of metaphase spindle throughout the movie and found two peaks of intensity (supplementary material Fig. S2G). The first peak corresponds to the accumulation of GFP signal in the midzone of the anaphase spindle (between 34 and 59 minutes from the start of the movie in supplementary material Fig. S2G,I, time point 35′46″) and the phragmoplast (supplementary material Fig. S2I, time point 41′56″). A similar cell is shown in supplementary material Fig. S2E. Optical sectioning of a cytokinetic cell showed that GFP-Lifeact staining accumulated at the midzone of the outer (expanding) edge of the phragmoplast (supplementary material Fig. S2H, top row) where it colocalised with the newly formed cell plate. The remainder of the phragmoplast was stained evenly (supplementary material Fig. 2C, middle and bottom rows), with a typical clear zone where the cell plate is formed. The second peak of GFP signal intensity corresponded with the association of the actin with the cell wall between daughter cells after cytokinesis is complete (between 70 and 95 minutes in supplementary material Fig. S2G and time point 78′56″ in supplementary material Fig. S2I). A similarly staged cell is shown in supplementary material Fig. S2F, where GFP-Lifeact associated with the newly formed cell wall. Notably, the GFP signal did not associate with the mother cell walls at this time point.

Dynamics of F-actin is tissue specific

Time-lapse imaging of cells expressing GFP-Lifeact demonstrated active rearrangements of F-actin. Two mechanistically distinct types of dynamics were observed. One characterised by elongation, severing and shortening events (supplementary material Movies 3 and 4), and the second by elastic contraction-like rearrangements, which occur via bundling, unbundling, stretching and retraction (supplementary material Movie 5). Both types were observed in stably transformed *A. thaliana* plants and BY-2 cell lines, but the second mechanism clearly predominated in the transiently transfected leaves of *N. benthamiana*.

Tracking of individual filaments in *A. thaliana* leaf pavement cells showed that initiation of the filament is followed by a short phase of rapid elongation (Fig. 1A), with a subsequent latent phase, when the length of a filament undergoes minor fluctuations (Fig. 1B). The filament was eventually severed and disappeared. Sometimes elongation of a filament resulted in bending, perhaps as a result of spatial crowding or attachments at the filament ends

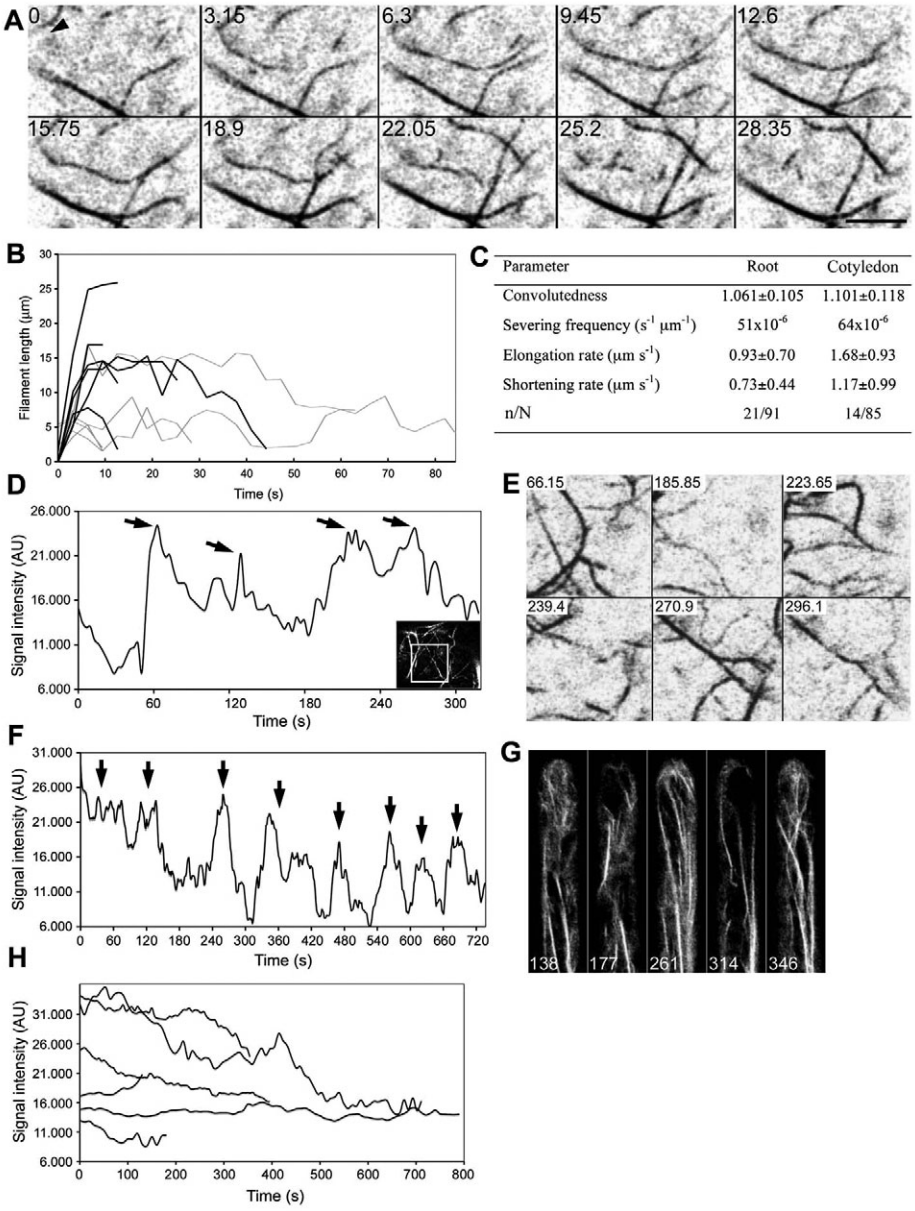

Fig. 1. Dynamics of actin filaments.
(**A**) Sequential time-lapse frames of a cotyledon cell. Within 28 seconds, the filament indicated by the arrowhead in the first frame elongates, is severed at least four times and disappears. Images are 2-μm-thick optical sections of the cortical layer of cytoplasm. Scale bar: 5 μm. (**B**) Plot showing time-dependent fluctuation of the length of six representative filaments from each of a cotyledon cell (black lines) and a root cell (grey lines). (**C**) Comparison of the dynamics and convolutedness of F-actin in cotyledon and root cells. (**D**) Periodic fluctuations of the GFP signal in a cotyledon cell measured in the area outlined by the white square in the inset. The arrows here and in F denote the peaks of the GFP signal. (**E**) Selected frames from the movie measured in D; the numbers represent the corresponding time points. (**F**) Periodic fluctuations of the GFP-Lifeact signal at the tip of a non-growing root hair. (**G**) Selected frames from the movie used to measure the GFP signal in F. Numbers indicate the corresponding time points. Note the correlation between the peaks and troughs on the chart with the images. (**H**) GFP signal measured in six separate cells expressing GFP-tubulin. Note that the changes in the signal are not periodic.

(supplementary material Fig. S3). The severing is likely to occur at the sites of bending. This high dynamicity was typical of the majority of filaments; however, both supplementary material Movies 3 and 4 show several very bright, presumably thicker, filaments that reorganise much more slowly. To analyse the behaviour of these filaments, we recorded time-lapse movies of image stacks representing the whole optical depth of root epidermal cells (supplementary material Movie 11). Fine filaments in this movie are not likely to be resolved because of the slow speed of image acquisition (86 seconds/frame). Analysis of the movie demonstrated that the brighter or thicker filaments showed slower dynamics, but that these dynamics were similar to all other filaments in that they also underwent elongation and severing (supplementary material Fig. S4A), bundling and stretching. In addition, these filaments could split into several thinner filaments at a fork that migrated along the filament (supplementary material Fig. S4B).

To compare the dynamic behaviour of filaments in different cell types, we traced the length of filaments in pavement cells of 10-day-old cotyledons and epidermal cells of 4-week-old roots and plotted the data for six representative examples in Fig. 1B. Both cell types had short-lived filaments that disappeared within 15 seconds of origin and filaments that persisted for longer. Root epidermal cell filaments generally persisted the longest. We compared severing frequency, elongation and shortening rates, and convolutedness [the degree of filament bending which is relative to the ratio of filament length to the length of a straight line joining its ends (Staiger et al., 2009)] of these filaments and conclude that actin is more dynamic in cotyledon pavement cells (Fig. 1C; supplementary material Fig. S5). The filaments in cotyledon pavement cells elongated and shortened faster and were severed more frequently. The convolutedness of filaments in the same cells was also higher (Student's *t*-test, $P<0.05$). The growth rate of filaments in both cotyledon pavement cells and root epidermal cells showed a high degree of variability.

The density of microfilaments in Fig. 1A increased from frame 0 to frame 22.05 and decreased subsequently. We investigated this

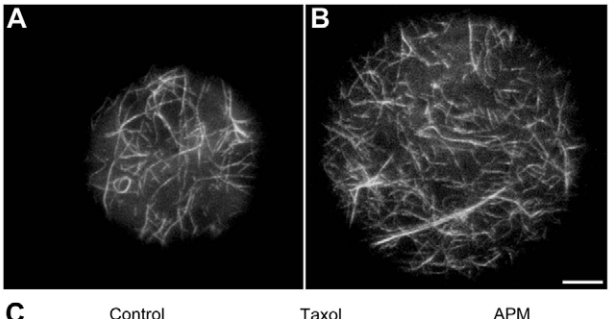

C

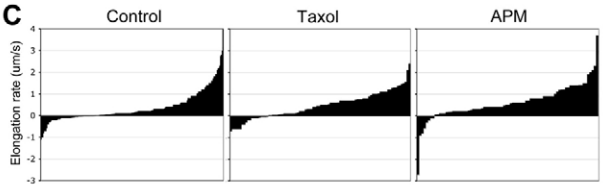

D

Treatment	Elongation (μm s^{-1})	Shortening (μm s^{-1})	n/N
Control	0.59±0.69	-0.19±0.25	22/173
APM	0.76±0.63	-0.71±0.86	20/72
Taxol	0.67±0.50	-0.28±0.24	20/70

Fig. 2. Microtubule dynamics influences F-actin dynamics. (**A**,**B**) Two images exemplifying the filamentous and spiky F-actin organisation in the cortical cytoplasm of protoplasts isolated from BY-2 cells. TIRF images with a 90 nm penetration depth of the evanescent wave. Scale bar: 5 μm. (**C**) Charts showing the distribution of F-actin growth rates in control and taxol- and APM-treated protoplasts. (**D**) Comparison of growth and shortening rates of filaments from control and taxol- and APM-treated samples. n and N denote the number of filaments analysed and the number of measurements, respectively.

phenomenon in several separate cells and found that the GFP signal fluctuated with a periodicity of 70.4±17.7 seconds (n=5; Fig. 1D,E). Similar periodic fluctuations were observed in root hairs (Fig. 1F,G) and these occurred independently of root hair elongation, because the periodicity of the signal in growing root hairs and non-growing root hairs was similar; 67.8±20.1 seconds (n=5) and 79.2±22.4 seconds (n=4), respectively. This periodicity appeared to be unique to the actin cytoskeleton, because the GFP-tubulin signal, when measured in a similar way, showed no periodic fluctuations (Fig. 1H).

Microtubules influence dynamics of F-actin

Microfilaments and microtubules have complementary roles in cells and are interconnected by a set of crosslinking proteins (Petrasek and Schwarzerova, 2009). Drug-induced depolymerisation of microtubules affects the organisation of microfilaments and vice versa, indicating that interplay between the different filament networks coordinates their dynamic behaviour (Collings, 2008). The question we wanted to address was whether the actin dynamics we describe above are dependent on microtubules. We measured the dynamics of GFP-Lifeact-labelled cortical F-actin in BY-2 cell protoplasts treated with the microtubule-depolymerising drug amiprophos-methyl (APM) and the microtubule-stabilising drug taxol compared with carrier compound (0.1% DMSO) as a control. We chose BY-2 cell protoplasts for this study because of the uniform effect of these drugs in single cells compared with whole tissues and we imaged filaments using TIRF (Fig. 2A,B; supplementary material Movie 6). In the protoplasts, F-actin was present as either long filaments, or short spikes. Both types of filament could be stable or dynamic similarly to the actin filaments in cotyledon pavement cells and root epidermal cells. No significant differences were found between the growth rates of long and short F-actin, except that the elongation phase of the short filaments terminated sooner. Generally, the filament growth rate was slightly slower in the protoplasts compared with the filaments in the cotyledon pavement and root epidermal cells, whereas shrinkage was three- to fivefold slower (compare Fig. 1C with Fig. 2D).

Treatment with Taxol or APM increased the proportion of faster-growing filaments, as shown by the decrease in the curvature of the growth-rate charts compared with the control (Fig. 2C). The average filament-elongation rate of APM-treated protoplasts was 30% faster than in the control (Student's t-test P<0.05; Fig. 4D), whereas the difference between taxol-treated protoplasts and the control was not significant (P>0.05). Neither treatment had a statistically significant effect on the filament convolutedness. These data demonstrate that the depolymerisation of microtubules leads to faster elongation and shortening of actin filaments, whereas stabilisation of microtubules had no effect on actin filament dynamics.

Mechanisms of the reorganisation of the F-actin network

Elongation, bundling, severing and shrinkage events underlie the stochastic nature of F-actin rearrangements in the cell (Michelot et al., 2007; Staiger et al., 2009). Our detailed analysis of time-lapse images reveals an additional mechanism for the reorganisation of the microfilament network. In four consecutive frames shown in Fig. 3A three filaments (marked by the arrowheads in the frame 0) combined into a longer filament, which later associated with other filaments, establishing a new cluster. Therefore, new filaments can originate and elongate via a combination of the existing shorter fragments. New filaments can also be constructed by the joining of free ends of severed fragments. The selection of frames from supplementary material Movie 3 shown in Fig. 3B illustrates the formation of new filaments from several (colour-traced) progenitors. This process appeared to rely on the filaments capturing each other's ends. TIRF of protoplasts revealed that some filaments have fine distal protrusions, which can either thicken, thus contributing to the elongation of the filament (Fig. 4A), or bundle with surrounding filaments (Fig. 4B). This might provide the mechanism for the joining of ends that we showed in Fig. 3A. We suggest that these protrusions represent single actin filaments that can link different fibres together, thus directing filament reorganisation. Quantification of the intensity of fluorescence of these fine filaments and brighter fibres suggests that F-actin bundles in protoplasts are formed by 13±5 filaments.

In conclusion, the majority of filaments brightly labelled with GFP-Lifeact represent bundles of eight and more individual filaments. The growth of these bundles depends on the elongation rate of individual filaments at the end of the bundle as well as end-association of pre-existing filaments. Considering the stochastic nature of this process, we would expect high variability of the rates of individual filament elongation, which is evident in Fig. 1C and supplementary material Fig. S5.

Characterisation of actin quoit-like structure

GFP-Lifeact also revealed coiled-like structures in BY-2 cells in all plant tissues examined, except growing root hairs (Fig. 5A-D; supplementary material Fig. S5). To distinguish these structures

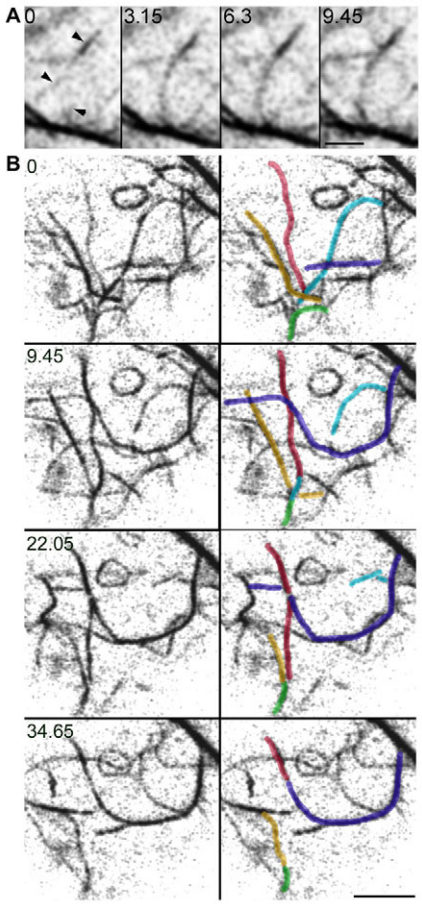

Fig. 3. Reorganisation of the F-actin network by rearrangement of existing filaments. (**A**) Four sequential time-lapse frames showing the formation of a filament by capture and end-joining. Three shorter filaments (indicated by the arrowheads) are bundled to produce one long bundle in root cell. Thereafter, the intensity of this filament increases. Scale bar: 2 µm. (**B**) Four sequential time-lapse frames demonstrating that new F-actin filaments can be formed by severing and end-joining of the existing filaments. Individual filaments have been colour-traced (panels on right). In this example one filament can be made from as many as three progenitors. Scale bar: 5 µm. All images were captured by CLSM.

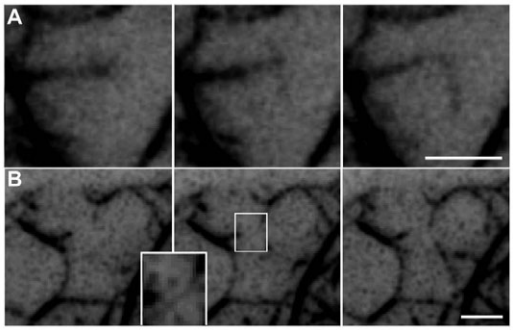

Fig. 4. TIRF microscopy images of fine actin structures in BY-2 cell protoplasts. (**A**) Two fine filaments originate from the end of the thick fibre (left panel). In the subsequent frames (middle and right panels), one of these defines the direction of fibre elongation (1 second per frame). (**B**) A fine filament protrudes from the end of a growing bundle in the second frame (middle). This filament is bundled with a neighbouring one to produce a long bent bundle in the third frame (right). Rate: 1.4 seconds per frame. Scale bars: 2 µm.

from actin rings in animal and yeast cells, we propose the term actin quoit-like structures or 'acquosomes'. Nomarski microscopy showed that acquosomes exist as independent disk-shaped organelles (Fig. 5C; supplementary material Movie 7) of variable diameter measured at 3.5±1.2 µm, except in non-growing root hairs, where the diameter was 1.6±0.3 µm. Normally cytoplasmic, acquosomes were also detected in nuclei (Fig. 5B). The acquosomes could oscillate around a concise area, or move for long distances, as observed in root hairs (Fig. 5D,G; supplementary material Movies 3 and 8). They were more resistant to Cytochalasin D than the rest of the filaments, but were sensitive to Latrunculin B (Fig. 6A,B).

Interphase and M-phase BY-2 cells contained ~6.7 acquosomes, but in some cases, up to 30 individual structures could be found in cells. We calculated the number of acquosomes per square millimetre of cell area (Fig. 6E) and found that BY-2 cells have 10,000 times more acquosomes than the cells we examined in *Arabidopsis*. Most BY-2 cells proliferate, whereas the cells in differentiated plant tissues rarely divide. Therefore the massive difference in the number of acquosomes might be attributable to the mitotic activity of the cells. To check this, we withdrew the growth regulator auxin from the BY-2 cell culture medium to reduce cell division and promote cell elongation. In doing so, the number of acquosomes was reduced by 98.8% (Fig. 6D,E).

We observed two routes to acquosome formation. The first was by coiling, as exemplified in Fig. 5F,G (supplementary material Movies 3, 9 and 10). In this case, one or more filaments underwent several rounds of coiling, as a result, the intensity of the ring fluorescence increased with each turn. The second was by circularisation of one or more straight filaments as exemplified in Fig. 6E. In either case the formation of the rings was a dynamic process that might involve the sliding of actin filaments. To determine whether this filament sliding was dependent on myosin activity, we treated BY-2 cells with 50 mM BDM. After 2 hours, we noted a 91.9% reduction in the frequency of rings (Fig. 6C,E). Treatment of cells with the anti-microtubular drug Amiprophosmethyl (20 µM), the membrane-trafficking inhibitor Brefeldin A (0.1 mM), the protein phosphatase I and II inhibitor Okadaic acid (0.4 nM), the cyclin-dependent kinase inhibitor Olomoucine (100 µM), the general protein kinase inhibitor Staurosporine (10 µM), the calmodulin inhibitor W7 (250 µM) and the phosphatidylinositol 3-kinase inhibitor Wortmannin (20 µM) had no effect on acquosome morphology and abundance. The disassembly of acquosomes involved multiple severing events (Fig. 5G; supplementary material Movies 3 and 10) or a ring opening and unfolding event (Fig. 5E). The acquosomes have also been observed in *A. thaliana* plants transformed with GFP-fABD (supplementary material Fig. S6; supplementary material Movie 10), indicating that F-actin coiling is independent of the visualisation probe used.

Discussion

Lifeact as a marker

The Lifeact peptide is a 17 amino acid sequence derived from the budding yeast actin-binding protein Abp140. Translational fusions of this peptide with fluorescent proteins results in the decoration of actin filaments when expressed in yeast, vertebrate and plant

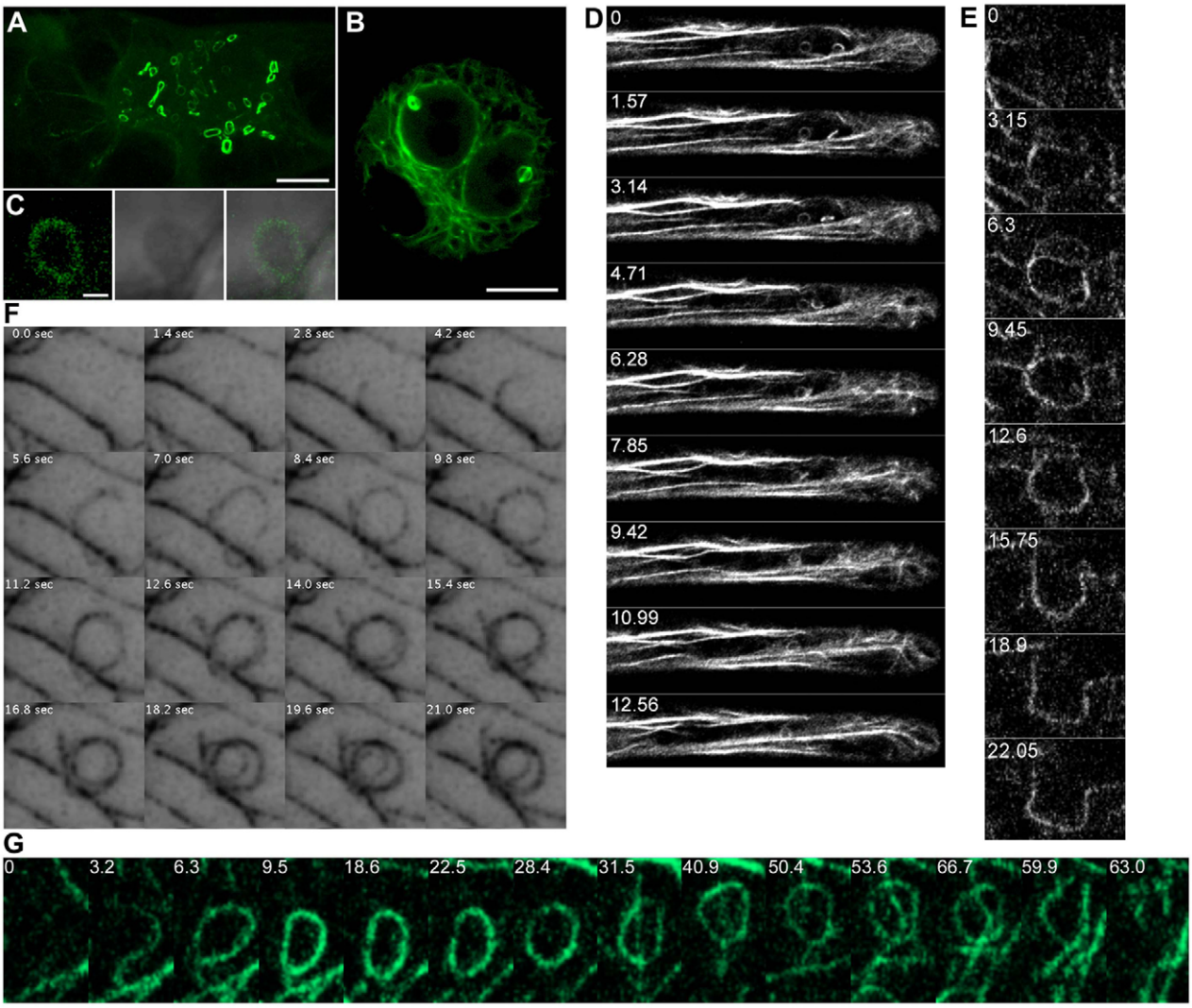

Fig. 5. Acquosomes are independent, mobile and dynamic structures. (**A**) Maximum projection of an interphase BY-2 cell. Many of the quoit-like structures are concentrated at the centre of the cell. Scale bar: 10 µm. (**B**) Multi-nucleate protoplast with acquosomes located inside two of the nuclei. Single optical section. Scale bar: 10 µm. (**C**) Acquosomes are structurally independent organelles; differential-interference contrast (DIC) and single optical section fluorescence images of BY-2 cell. Scale bar: 2 µm. (**D**) Acquosomes are mobile. Subsequent frames from supplementary material Movie 8 showing the movement of acquosomes inside a root hair. (**E**) An example of a short-lived acquosome that unfolds several seconds after formation. The unravelling of this acquosome occurs after one severing event, but does not lead to the disassembly of the actin filament from which it was formed. (**F**) Sequential images acquired by TIRF microscopy demonstrating acquosome formation. (**G**) Time frames showing the formation and dissolution of an aquosome taken from supplementary material Movie 3. Note that several severing events occur during the dissolution stage in frames '59.85' and '63.0' resulting in the complete disappearance of the acquosome. The frame '0' in the image corresponds to frame '1:12' in the movie.

cells (Riedl et al., 2008; Vidali et al., 2009; Era et al., 2009). In this paper, we have demonstrated that GFP-Lifeact is a useful marker for studying the dynamics of fine actin filaments and rearrangements of bundles in stably transformed plants and cell lines. Lifeact has no discernible effect on plant growth and development (Era et al., 2009) or cell cycle progression. Here, we have shown, using Lifeact as the probe, that actin filaments elongate, bundle or undergo severing. Similar actin dynamic events have been demonstrated in plants expressing GFP-fABD (Staiger et al., 2009). Filament growth rates, severing frequencies and the degrees of convolutedness in lines expressing GFP-Lifeact and GFP-fABD are similar. However, Lifeact and fABD have different kinetics of binding to F-actin in vivo, as determined by FRAP analysis. The rate of GFP-fABD turnover was measured to be 13.2±1.3 seconds (Sheahan et al., 2004). Similar values have been shown for GFP-talin (Sheahan et al., 2004) and GFP-WLIM1 (Thomas et al., 2006). By contrast, the GFP-Lifeact turnover was fourfold faster (2.56±0.70). The faster exchange rate indicates a different binding interaction with F-actin and suggests that Lifeact is a better probe for resolving fast events of actin organisation.

During cell cycle progression in tobacco tissue culture cells, Lifeact detects arrays and structures similar to those previously observed with fluorescently labelled phalloidin and fABD (Clayton and Lloyd, 1985; Schmit and Lambert, 1987; Traas et al., 1987; Zhang et al., 1993; Sano et al., 2005) and therefore is a suitable marker for labelling interphase and mitotic actin structures. In

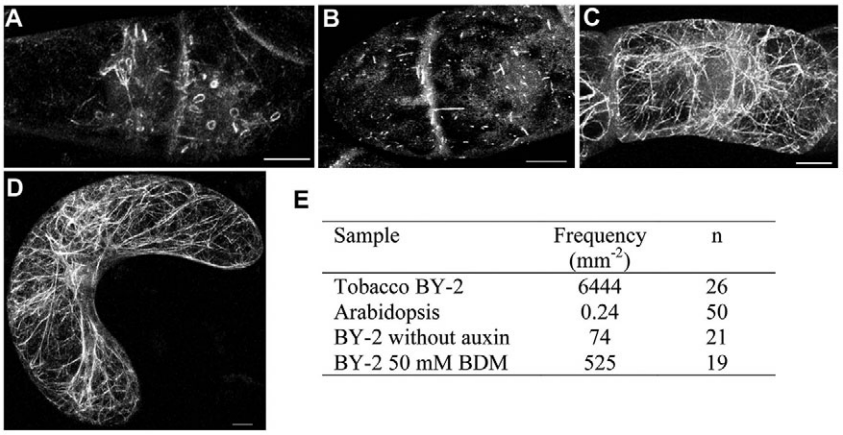

E

Sample	Frequency (mm^{-2})	n
Tobacco BY-2	6444	26
Arabidopsis	0.24	50
BY-2 without auxin	74	21
BY-2 50 mM BDM	525	19

Fig. 6. Analysis of acquosomes. (**A-C**) Effect of Cytochalasin D (A), Latrunculin B (B) and BDM (C) on the acquosomes. (**D**) Organisation of microfilaments in BY-2 cell cultivated in the absence of auxin for 14 days. (**E**) Frequency of acquosomes in different samples expressed as number of structures per square millimetre of cell area. Scale bars: 10 μm.

addition, we could see enrichment of the signal in the midzone at the distal edge of the phragmoplast. This enrichment implies that the actin cytoskeleton is important at the point where microtubules and the membrane coordinate synthesis of the cell plate. We also detected a second wave of actin enrichment at the cell plate 10 minutes after phragmoplast disassembly, where it might be involved in the further maturation of the cell plate. Other proteins are known to associate with the cell plate after the disassembly of phragmoplast microtubules. For example, dynamin-like proteins are essential for cell plate formation and accumulate in the midzone after anaphase as the cell plate initiates and then follows the expanding edge of the phragmoplast. Dynamin remains associated with the cell plate after the disassembly of phragmoplast microtubules during maturation of the cell plate (Kang et al., 2003). Perhaps actin supports dynamin-dependent processes at this stage.

Actin dynamics in different cell types

Plant cells can grow isotropically or anisotropically. It is known that the organisation of F-actin is different in isotropic and anisotropic cells, with the networks being more random in isotropic cells (e.g. in leaf epidermal and mesophyl cells) compared with anisotropic cells (e.g. root or hypocotyl epidermal cells) (Kotzer and Wasteneys, 2006). Here, we show that the dynamics of the actin networks is different within these cells. We chose to compare isotropically growing cotyledon pavement cells with anisotropically growing root epidermal cells from the elongation zone. We noted that the pavement cells contained a more dynamic and convoluted F-actin array than the root epidermal cells, where a more ordered actin array of straight filaments was observed. This type of network typically had reduced F-actin growth and shortening rates. Interestingly, growing and non-growing anisotropic cells of the same type, i.e. hypocotyl epidermal cells, have been shown to have similar filament convolutedness, severing frequency and elongation rate, indicating that growth is independent of the rate of actin dynamics (Staiger et al., 2009). Isotropic cell expansion is therefore accompanied by increased dynamics of actin filaments.

A notable feature of the growth of F-actin has been the fluctuations in the length of the filaments as described in Fig. 1B. The filaments appear to shorten randomly before they re-grow and we have determined a shortening rate to describe this phenomenon. We have included such values as a parameter to describe the dynamics of the filaments. This shortening could occur by severing of the filaments, with the concurrent loss of the fragment by cytoplasmic streaming, or by disassembly at the filament ends and filament sliding. The shortening rate was lower in root epidermal cells compared with cotyledon pavement cells, which was consistent with the difference in elongation rates between the two cell types.

Mechanisms of actin network reorganisation

Reorganisation of the actin network occurs via two distinct mechanisms that co-exist in time. The first relies on the formation of new filaments and the severing or shortening of existing filaments. This type of F-actin reorganisation has been called stochastic dynamics and is dependent on myosin activity for the severing events, but not for the elongation events, and has been observed in the cortical layer of cytoplasm (Michelot et al., 2007; Staiger et al., 2009). Dynamic instability is typical for microtubules, where individual filaments can elongate or shrink at the end, but has not been observed for F-actin, perhaps because actin-bundling proteins can stabilise filaments and prevent their disassembly. Severing therefore appears to be the major mechanism of modulation of F-actin network organisation. Severing of fibres can occur in several places within a short space of time, generating numerous smaller fragments that are moved by cytoplasmic streaming or diffusion, resulting in the disassembly of the entire structure. According to the current model, these fragments break down to G-actin, which can then be recycled for the polymerisation of new filaments. The disassembly of the fragments has never been proven, although there is always a pool of G-actin in the cytoplasm. The majority of actin fragments cannot initiate new filaments, suggesting that the barbed ends are capped by gelsolin-like activity (Staiger et al., 2009). This capping of filaments is essential for keeping a low-density network, because rapid generation of barbed ends in the presence of a high concentration of free actin in plant cells can lead to a dense lamellipodia-like network. We have noted that the inhibition of filament polymerisation at the severed ends is not always very efficient and occasionally fine protruding filaments can be observed at the ends. These filaments could result from the elongation of existing free barbed ends or from the formation of new filaments generated by proteins, such as the *Arabidopsis* non-processive formin AtFH1, along the length of existing filaments (Michelot et al., 2006). The protrusions can capture and crosslink several filaments, resulting in the rearrangement of the entire actin network without bulk polymerisation, bundling or sliding events.

The second mechanism does not require formation of new filaments and involves filament bundling, unbundling and sliding

events in continual dynamic rearrangement. Similar behaviours of actin networks have been observed previously in *Arabidopsis* and moss cells (Staiger et al., 2009; Era et al., 2009). Treatment with BDM inhibits the sliding, suggesting that myosin has a role. This sliding is typical of thick actin cables within cytoplasmic strands, as well as in the cortical cytoplasm. Apart from this dynamic rearrangement, the behaviour of actin cables exhibits features of stochastic dynamics with characteristic buckling, elongation and severing events.

Evaluation of the intensity of fluorescence from individual fibres rendered a range of values. If we assume that fibres with the lowest value are single filaments, it is possible to estimate that an average actin bundle is made of 8–18 single filaments. The fine filaments can attach to existing filament end(s) or be free in the cytoplasm. Each frame in the time-lapse sequence presents a different arrangement of these filaments, making their tracking very difficult. This is either because of the rapid dynamics of the filaments or because of their movement by cytoplasmic streaming or diffusion. However, as single filaments are rapidly moved around a cell, they can potentially act as structural blocks that can cause rapid elongation of filaments upon capture by free ends. This association can occur via bundling proteins such as villin and fimbrin, or independently, by direct binding of the filaments as observed previously (Michelot et al., 2007). This type of elongation at the free ends of actin filaments might provide an explanation of the fast growth rates of F-actin observed in plant cells (fastest average 1.68 μm/second) compared with that in vitro or in *Schizosaccharomyces pombe* (0.2 μm/second) (Michelot et al., 2007; Vavylonis et al., 2008) or in lamellipodia (0.5 μm/second) (Ponti et al., 2004). Inhibition of myosin activity by BDM does not affect the elongation rate of actin filaments (Staiger et al., 2009), indicating that protrusions at the end of the fibres, as well as their rapid elongation, are not a result of filament sliding. Moreover, the shrinkage rate of actin filaments in plant cells was observed to be 1.17 μm/second. The fastest shrinkage of F-actin in vitro has been observed when cofilin is added and is 0.03 μm/second; without cofilin the rate was only 0.008 μm/second (Andrianantoandro and Pollard, 2006), indicating that in vivo, other factors controlling shrinkage must be involved.

With these data in mind, it is possible to describe a strategy for actin reorganisation based on our observations. In this strategy, actin filaments polymerise randomly in the cytoplasm and these can be bundled with similar filaments, resulting in thicker and longer bundles composed of staggered filaments of random length. This bundling results in an elastic network that is capable of undergoing light rearrangements via filament unbundling or sliding. A significant rearrangement requires severing events that create unattached fragments of different length. Shorter fragments migrate in the cytoplasm by diffusion or cytoplasmic flow and can depolymerise or join other filaments. Some longer filaments do not move, but join with neighbouring longer filaments or moving shorter fragments. The proportion of filaments that undergo depolymerisation or join existing filaments is so far not possible to estimate, but the balance can change depending on the physiological condition of the cell.

Interestingly, stabilisation of microtubules has no significant effect on actin dynamics, indicating that microtubules neither obstruct microfilament elongation, nor prevent diffusion of the shorter structural elements. However, depolymerisation of microtubules induced an increase in both the actin polymerisation and depolymerisation rates, indicating that actin dynamics is modulated by microtubules. These data demonstrate that the dynamics of F-actin depends on the integrity of the microtubule network, providing compelling evidence of the interplay between both filament systems.

Furthermore, the density of the actin filaments in root cells and in cotyledons follows a periodicity that is not seen when we follow the density of microtubules. These data strongly suggest that actin filament dynamics are regulated in an oscillatory manner that might reflect fluctuations of ionic environments, which directly or indirectly regulate actin filament growth and shortening. In this context, it has been shown that oscillatory dynamics of ions and ion transporters in root and leaf cells can affect growth parameters such as cell size (Hepler et al., 2001; Shabala et al., 2006). In turn, the activity of many actin-regulating proteins is sensitive to the concentration of Ca^{2+} or H^{+} (reviewed in Hepler et al., 2001; Hussey et al., 2006) and therefore severing and bundling activities might contribute to this phenomenon.

Acquosome

Circular conformations of actin filaments have been observed in vegetative tissues and pollen tubes of evolutionary distant plant species, including Chara (Higashi-Fujime, 1980), tobacco, rice, *Vinka rosea* (Hasezawa et al., 1988; Wilsen et al., 2006), Zinnia (Frost and Roberts, 1996) and *Chenopodium* (Chaidee at al., 2008) using light microscopy (Higashi-Fujime, 1980), phalloidin-derived fluorescent probes (Hasezawa et al., 1988; Frost and Roberts, 1996; Chaidee at al., 2008) or GFP fusion of the actin-binding protein WLIM (Thomas et al., 2006), talin and fimbrin (Wilsen et al., 2008). We have observed identical conformations using fimbrin actin-binding domain GFP and GFP-Lifeact in all types of *Arabidopsis* cells examined and in BY-2 cells. Our data, taken together with previous observations, suggest that this is a bona fide actin-based organelle and we have named this an Acquosome.

Template- or organelle-independent circularisation was the first proposed mechanism of acquosome formation in cytoplasmic extracts from Chara cells (Higashi-Fujime, 1980) and we note the same mechanism in living cells. The end of an elongating or stationary filament starts curling, eventually making a coil, which then gains intensity of fluorescence as a result of the continued coiling of the mother filament. Resulting quoits represent a bundle of parallel filaments (Higashi-Fujime, 1980) made of up to 18 individual filaments judging by the intensity of GFP fluorescence, which indicates that actin-bundling proteins are involved in the formation. The quoits can form from F-actin bundles in vitro after the components of the cytoplasm have been replaced with a buffer, indicating that all required factors are located on the bundle and spontaneous or signal-induced changes in their activity leads to the curvature. A low concentration of Ca^{2+}, for example, can promote circularisation of the filaments (Higashi-Fujime, 1980; Chaidee at al., 2008). Although imaging has provided detailed information about spatial aspects of acquosome formation, the molecular mechanisms of this process remain poorly understood. Coiling seems to be an intrinsic feature of bundled F-actin that requires both myosin ATPase activity and bundling factors, because treatment with BDM reduces the number of acquosomes, but does not abolish them. We show that after the formation of acquosomes, which can take between 5 and 10 seconds, they can either persist or unfold immediately. In addition, they can be severed and disappear. When they persist, they can oscillate around one point, as is seen in BY-2 cells, or migrate around the cell, as seen in root hairs. The migration pattern in root hairs resembles the reciprocal

flow of the cytoplasm, suggesting that cytoplasmic streaming generates the propelling force.

An important question concerns the function of acquosomes. Many lines of evidence demonstrate a correlation between the number of acquosomes and the physiological status of the cell. For example, the frequency of rings or acquosomes decreases in an aging tobacco BY-2 cell culture (Hasezawa et al., 1988), increases during heat-stress (Chaidee at al., 2008) and following mechanical separation of Zinnia mesophyll cells (Frost and Roberts, 1996). We have observed a striking abundance of acquosomes in BY-2 cells compared with plant tissues, suggesting a positive correlation between cell proliferation and acquosome formation. The fact that the number of acquosomes is reduced by 98.9% when BY-2 cells are induced to elongate by auxin deprivation, and no acquosomes were observed in rapidly growing root hairs, strongly suggests that acquosomes provide a storage form of surplus actin. This storage form of actin will then be able to buffer the concentration of free actin and the number of filaments in the cytoplasm, so that rapid release of this material is possible when required for organisation of the actin cytoskeleton during cell elongation.

Materials and Methods

Generation of *A. thaliana* and BY-2 lines expressing GFP-Lifeact

A synthetic gene corresponding to the Lifeact peptide sequence (Riedl et al., 2008) was produced from two overlapping oligonucleotides 5′-GGGGACAAGTTTG-TACAAAAAAGCAGGCTTCATGGGTGTTGCTGATCTTATTAAGAAGTTCGA-GTCTATTTC-3′ and 5′-GGGGACCACTTTGTACAAGAAAGCTGGGTCTTC-CTCCTTAGAAATAGACTCGAACTTCTTAATAAGATCAGC-3′, using one cycle reaction with *Taq* polymerase (Biomol) according to the manufacturer's recommendations. The resulting gene was cloned into Gateway entry vector pDonr207 (Invitrogen) and then into the pMDC43 binary vector (Curtis and Grossniklaus, 2003). The constructs were transformed into *Agrobacterium tumifaciens* strain C58C3 for transformation of *A. thaliana* plants and into strain LBA4404 for transformation of tobacco BY-2 cells. *A. thaliana* plants were transformed by the floral dip method (Clough and Bent, 1998), BY-2 cells were transformed by the co-incubation method (Geelen and Inze, 2001). To select transformed plants, seeds were sterilised in 1% bleach for 10 minutes, washed twice in sterile water, vernalised for 2 days at 4°C and planted on half-strength Murashige and Skoog's basal salt medium supplemented with 1% sucrose, 0.7% agar and 50 mg/l Hygromycin B. Transgenic BY-2 lines were selected on normal growth medium supplemented with 0.7% agar, 500 mg/l carbenicillin and 40 mg/l Hygromycin B. Carbenicillin was withdrawn from the medium after four passages.

Growth of plant material and protoplast isolation

N. tabacum BY-2 cells were grown in liquid culture and protoplasts were isolated as described (Jiang and Sonobe, 1993). *A. thaliana* seeds were sterilised and grown as described above.

Imaging

Confocal microscopy images were acquired using a Leica SP5 or a Zeiss 510 meta system. For the root imaging, seeds were sterilised and vernalised as described above, and planted on half-strength Murashige and Skoog's basal salt medium supplemented with 1% sucrose and 0.7% agarose in Petri dishes containing a glass coverslip (Iwaki). The images were recorded whilst the roots were growing along the coverslip. TIRF microscopy images were acquired using a Leica system equipped with a HCX PL Apo 100×/1.46 TIRF objective and a Hamamatsu 9100-02EMCCD camera. The evanescent wave penetration depth was between 70 and 110 nm.

DNA and the cell plate were stained with the red component of the Total Nuclear-ID Green-Red Nucleolar/Nuclear Detection kit (Enzo Life Sciences). The dye was added to the tissue culture medium at a dilution of 1:500 and images were taken after incubation for 15 minutes using a Cy5 filter.

The quantification of the images was performed using ImageJ. In all charts showing intensity of GFP, the background values were measured in the area of the cell lacking any visible filaments and subtracted from the plotted signal. The FRAP experiments were performed and quantified as described (Chang et al., 2005). To quantify the thickness of actin bundles, it was assumed that the Lifeact-GFP fluorescence signal level is proportional to the amount of actin located within the filament. The absolute signal of each filament in the cells was measured and all signals were ranked. The filaments with the lowest intensity were assumed to be single filaments and the GFP fluorescence signal of other filaments was divided by this intensity to give the number of single filaments in the bundle.

Drug treatments

Taxol and amiprophos methyl were used at a final concentration of 20 μM. The 20 mM stock solutions were prepared in DMSO. The control samples were supplemented with 0.1% DMSO. The stock solutions of 0.5 M 2,3-butanedione monoxime (BDM) and 125 mM N-(6-aminohexyl)-5-chloro-1-naphthalenesulfonamide (W-7) were prepared in water. Stock solutions of 10 mM Cytochalasin D, 1 mM Latrunculin B, 50 mM Brefeldin A, 25 mM Olomoucine, 10 mM Staurosporine and 10 mM Wortmannin were prepared in DMSO. The stock solution of 0.2 mM okadaic acid was prepared in ethanol.

We thank the Biotechnology and Biological Sciences Research Council, UK for funding (BB/E006256/1).

Supplementary material available online at
http://jcs.biologists.org/cgi/content/full/123/17/3019/DC1

References

Andrianantoandro, E. and Pollard, T. D. (2006). Mechanism of actin filament turnover by severing and nucleation at different concentrations of ADF/cofilin. *Mol. Cell* **24**, 3-23.

Chaidee, A., Foissner, I. and Pfeiffer, W. (2008). Cell-specific association of heat shock-induced proton flux with actin ring formation in *Chenopodium* cells: comparison of auto- and heterotroph cultures. *Protoplasma* **234**, 33-50.

Chang, H.-Y., Smertenko, A. P., Igarashi, H., Dixon, D. P. and Hussey, P. J. (2005). Dynamic interaction of NtMAP65-1a with microtubules in vivo. *J. Cell Sci*. **118**, 3195-3201.

Clayton, L. and Lloyd, C. W. (1985). Actin organization during the cell cycle in meristematic plant cells. Actin is present in the cytokinetic phragmoplast. *Exp. Cell Res.* **156**, 231-238.

Clough, S. J. and Bent, A. F. (1998). Floral dip: a simplified method for *Agrobacterium*-mediated transformation of *Arabidopsis thaliana*. *Plant J.* **16**, 735-743.

Collings, D. A. (2008). Crossed-wires: interactions and cross-talk between the microtubule and microfilament networks in plants. In *Plant Microtubules, Development and Flexibility* (ed. P. Nick), pp. 47-82. Berlin, Heidelberg, New York: Springer.

Curtis, M. D. and Grossniklaus, U. (2003). A gateway cloning vector set for high-throughput functional analysis of genes in planta. *Plant Physiol*. **133**, 462-469.

Deeks, M. J., Fendrych, M., Smertenko, A., Bell, K. S., Oparka, K., Cvrcková, F., Zársky, V. and Hussey, P. J. (2010). The plant formin AtFH4 interacts with both actin and microtubules, and contains a newly identified microtubule-binding domain. *J. Cell Sci.* **123**, 1209-1215.

Desai, A. and Mitchison, T. J. (1997). Microtubule polymerization dynamics. *Annu. Rev. Cell Dev. Biol.* **13**, 83-117.

Era, A., Tominaga, M., Ebine, K., Awai, C., Saito, C., Ishizaki, K., Yamato, K. T., Kohchi, T., Nakano, A. and Ueda, T. (2009). Application of lifeact reveals F-Actin dynamics in *Arabidopsis thaliana* and the liverwort, *Marchantia polymorpha*. *Plant Cell Physiol*. **50**, 1041-1048.

Frost, A. O. and Roberts, A. W. (1996). Cortical actin filaments fragment and aggregate to form chloroplast-associated and free F-actin rings in mechanically isolated *Zinnia* mesophyll cells. *Protoplasma* **194**, 195-207.

Fu, Y., Wu, G. and Yang, Z. B. (2001). Rop GTPase-dependent dynamics of tip-localized F-actin controls tip growth in pollen tubes. *J. Cell Biol.* **152**, 1019-1032.

Geelen, D. N. V. and Inze, D. G. (2001). A bright future for the BrightYellow-2 cell culture. *Plant Physiol*. **127**, 1375-1379.

Hasezawa, S., Nagata, T. and Syono, K. (1988). The presence of ring formed actin-filaments in plant-cells. *Protoplasma* **146**, 61-63.

Hepler, P. K., Vidali, L. and Cheung, A. Y. (2001). Polarized cell growth in higher plants. *Annu. Rev. Cell Dev. Biol.* **17**, 159-187.

Higaki, T., Kutsuna, N., Sano, T. and Hasezawa, S. (2008). Quantitative analysis of changes in actin microfilament contribution to cell plate development in plant cytokinesis. *BMC Plant Biol*. **8**, 80.

Higashi-Fujime, S. (1980). Active movement invitro of bundles of microfilaments isolated from *Nitella* cell. *J. Cell Biol.* **87**, 569-578.

Holweg, C. L. (2007). Living markers for actin block myosin-dependent motility of plant organelles and auxin. *Cell Motil. Cytoskeleton* **64**, 69-81.

Hussey, P. J., Ketelaar, T. and Deeks, M. J. (2006). Control of actin cytoskeleton in plant cell growth. *Annu. Rev. Plant Biol.* **57**, 109-126.

Ilgenfritz, H., Bouyer, D., Schnittger, A., Mathur, J., Kirik, V., Schwab, B., Chua, N. H., Jurgens, G. and Hulskamp, M. (2003). The Arabidopsis STICHEL gene is a regulator of trichome branch number and encodes a novel protein. *Plant Physiol.* **131**, 643-655.

Jiang, C. J. and Sonobe, S. (1993). Identification and preliminary characterization of a 65kDa higher-plant microtubule-associated protein. *J. Cell Sci.* **105**, 891-901.

Kang, B.-H., Busse, J. S. and Bednarek, S. Y. (2003). Members of the *Arabidopsis* Dynamin-like gene family, ADL1, are essential for plant cytokinesis and polarized cell growth. *Plant Cell* **15**, 899-913.

Ketelaar, T., de Ruijter, N. C. A. and Emons, A. M. C. (2003). Unstable F-actin specifies the area and microtubule direction of cell expansion in Arabidopsis root hairs. *Plant Cell* **15**, 285-292.

Ketelaar, T., Anthony, R. G. and Hussey, P. J. (2004). Green fluorescent protein-mTalin causes defects in actin organization and cell expansion in arabidopsis and inhibits actin

depolymerizing factor's actin depolymerizing activity in vitro. *Plant Physiol.* **136**, 3990-3998.

Kost, B., Spielhofer, P. and Chua, N. H. (1998). A GFP-mouse talin fusion protein labels plant actin filaments in vivo and visualizes the actin cytoskeleton in growing pollen tubes. *Plant J.* **16**, 393-401.

Kotzer, A. M. and Wasteneys, G. O. (2006). Mechanisms behind the puzzle: microtubule-microfilament cross-talk in pavement cell formation. *Can. J. Bot.* **84**, 594-603.

Lancelle, S. A. and Hepler, P. K. (1992). Ultrastructure of freeze-substituted pollen tubes of Lilium longiflorum. *Protoplasma* **167**, 215-230.

Mathur, J., Spielhofer, P., Kost, B. and Chua, H. H. (1999). The actin cytoskeleton is required to elaborate and maintain spatial patterning during trichome cell morphogenesis in Arabidopsis thaliana. *Development* **126**, 5559-5568.

Michelot, A., Derivery, E., Paterski-Boujemaa, R., Guerin, C., Huang, S. J., Parcy, F., Staiger, C. J. and Blanchoin, L. (2006). A novel mechanism for the formation of actin-filament bundles by a nonprocessive forming. *Curr. Biol.* **16**, 1924-1930.

Michelot, A., Berro, J., Guerin, C., Boujemaa-Paterski, R., Staiger, C. J., Martiel, J. L. and Blanchoin, L. (2007). Actin-filament stochastic dynamics mediated by ADF/cofilin. *Curr. Biol.* **17**, 825-833.

Miller, D. D., de Ruijter, N. C. A., Bisseling, T. and Emons, A. M. C. (1999). The role of actin in root hair morphogenesis: studies with lipochito-oligosaccharide as a growth stimulator and cytochalasin as an actin perturbing drug. *Plant J.* **17**, 141-154.

Petrasek, J. and Schwarzerova, K. (2009). Actin and microtubule cytoskeleton interactions. *Curr. Opin. Plant Biol*. **12**, 728-734.

Ponti, A., Machacek, M., Gupton, S. L., Waterman-Storer, C. M. and Danuser, G. (2004). Two distinct actin networks drive the protrusion of migrating cells. *Science* **305**, 1782-1786.

Qian, P., Hou, S. and Guo, G. (2009). Molecular mechanisms controlling pavement cell shape in Arabidopsis leaves. *Plant Cell Rep.* **28**, 1147-1157.

Riedl, J., Crevenna, A. H., Kessenbrock, K., Yu, J. H., Neukirchen, D., Bista, M., Bradke, F., Jenne, D., Holak, T. A., Werb, Z. et al. (2008). Lifeact: a versatile marker to visualize F-actin. *Nat. Methods* **5**, 605-607.

Sano, T., Higaki, T., Oda, Y., Hayashi, T. and Hasezawa, S. (2005). Appearance of actin microfilament 'twin peaks' in mitosis and their function in cell plate formation, as visualized in tobacco BY-2 cells expressing GFP-fimbrin. *Plant J.* **44**, 595-605.

Schmit, A.-C. and Lambert, A.-M. (1987). Characterization and dynamics of cytoplasmic F-actin in higher plant endosperm cells during interphase, mitosis, and cytokinesis. *J. Cell Biol*. **105**, 2157-2166.

Shabala, S., Shabala, L., Gradmann, D., Chen, Z., Newman, I. and Mancus, S. (2006). Oscillations in plant membrane transport: model predictions, experimental validation, and physiological implications. *J. Exp. Bot.* **57**, 171-184.

Sheahan, M. B., Staiger, C. J., Rose, R. J. and McCurdy, D. W. (2004). A green fluorescent protein fusion to actin-binding domain 2 of Arabidopsis fimbrin highlights new features of a dynamic actin cytoskeleton in live plant cells. *Plant Physiol.* **136**, 3968-3978.

Staiger, C. J., Sheahan, M. B., Khurana, P., Wang, X., McCurdy, D. W. and Blanchoin, L. (2009). Actin filament dynamics are dominated by rapid growth and severing activity in the Arabidopsis cortical array *J. Cell Biol.* **184**, 269-280.

Thomas, C., Hoffmann, C., Dieterle, M., Van Troys, M., Ampe, C. and Steinmetza, A. (2006). Tobacco WLIM1 is a novel F-actin binding protein involved in actin cytoskeleton remodeling. *Plant Cell* **18**, 2194-2206.

Traas, J. A., Doonan, J. H., Rawlins, D. J., Shaw, P. J., Watts, J. and Lloyd, C. W. (1987). An actin network is present in the cytoplasm throughout the cell cycle of carrot cells and associates with the dividing nucleus. *J. Cell Biol.* **105**, 387-395.

Vavylonis, D., Wu, J.-Q., Hao, S., O'Shaughnessy, B. and Pollard, T. D. (2008). Assembly mechanism of the contractile ring for cytokinesis by fission yeast. *Science* **319**, 97-100.

Vidali, L., Rounds, C. M., Hepler, P. K. and Bezanilla, M. (2009). Lifeact-mEGFP reveals a dynamic apical F-actin network in tip growing plant cells. *PLoS ONE* **4**, e5744.

Voigt, B., Timmers, A. C. J., Samaj, J., Muller, J., Baluska, F. and Menzel, D. (2005). GFP-FABD2 fusion construct allows in vivo visualization of the dynamic actin cytoskeleton in all cells of *Arabidopsis* seedlings. *Eur. J. Cell Biol.* **84**, 595-608.

Weerasinghe, R. R., Bird, D. M. and Allen, N. S. (2005). Root-knot nematodes and bacterial Nod factors elicit common signal transduction events in *Lotus japonicus*. *Proc. Natl. Acad. Sci. USA* **102**, 3147-3152.

Wilsen, K. L., Lovy-Wheeler, A., Voigt, B., Menzel, D., Kunkel, J. G. and Hepler, P. K. (2006). Imaging the actin cytoskeleton in growing pollen tubes. *Sex. Plant Rep.* **19**, 51-62.

Zhang, D., Wadsworth, P. and Hepler, P. K. (1993). Dynamics of microfilaments are similar, but distinct from microtubules during cytokinesis in living, dividing plant-cells. *Cell Motil. Cytoskeleton* **24**, 151-155.

Zhang, Y., He, J. M., Lee, D. and McCormick, S. (2010). Interdependence of endomembrane trafficking and actin dynamics during polarized growth of arabidopsis pollen tubes. *Plant Physiol.* **152**, 2200-2210.